

# Nonadiabatic effect in topological and interacting charge pumping

Fan Yang<sup>1</sup>, Xingyu Li, and Hui Zhai\*

*Institute for Advanced Study, Tsinghua University, Beijing 100084, China*

 (Received 24 August 2023; revised 8 January 2024; accepted 8 January 2024; published 2 February 2024)

Topological charge pumping occurs in the adiabatic limit, and the nonadiabatic effect due to finite driving velocity reduces the pumping efficiency and leads to deviation from quantized charge pumping. In this paper, we discuss the relation between this deviation from quantized charge pumping and the entanglement generation after a pumping circle. In the simplest setting, we show that the purity  $\mathcal{P}$  of the half-system reduced density matrix is equal to  $\mathcal{R}$ , defined as  $(1 - \kappa)^2 + \kappa^2$ , where  $\kappa$  denotes the pumping efficiency. In generic situations, we argue that  $\mathcal{P} < \mathcal{R}$  and the pumping efficiency can provide an upper bound for purity and, therefore, a lower bound for generated entanglement. To support this conjecture, we propose a solvable pumping scheme in the Rice-Mele-Hubbard model, which can be represented as a brick-wall-type quantum circuit model. With this pumping scheme, numerical calculation of charge pumping only needs to include at most six sites, and therefore the interaction and the finite-temperature effects can be both included reliably in the exact diagonalization calculation. The numerical results using the solvable pumping circle identify two regimes where the pumping efficiency is sensitive to driving velocity and support the conjecture  $\mathcal{P} < \mathcal{R}$  when both interaction and finite-temperature effects are present.

DOI: [10.1103/PhysRevB.109.064301](https://doi.org/10.1103/PhysRevB.109.064301)

## I. INTRODUCTION

Quantized transport is one of the most direct manifestations of nontrivial topology in quantum systems. It includes two different approaches. One is the quantized linear response to an external constant voltage field, including the quantized conductance in one-dimensional ballistic metals [1,2] and various kinds of quantum Hall effects [3–12]. Such measurements have been extensively used in condensed matter systems to probe topological phases. Generally speaking, this scheme requires a small voltage field such that the system remains in the linear response regime. The other is quantized charge transport in a dynamically driven process with periodic driving parameters [13–18]. The canonical example is the Thouless pump [14]. Such measurements can be more easily realized in ultracold atomic gases [19–24]. Generally speaking, this scheme requires a slow driving velocity such that the entire dynamic process remains within the adiabatic limit. In both cases, a small external field or slow dynamics is necessary for manifesting topology. Deviating from a linear response or the adiabatic limit inevitably causes deviation from topological quantization.

However, in practice, the driving speed is always finite in experiments, and consequently, the nonadiabatic effect results in a deviation from quantization. This deviation has been observed in a recent cold-atom experiment [24]. In this experiment, tunable interactions between particles were also presented. The sensitivity to finite driving speed depends on the interaction as well as the temperature. Previously, in the case of crossing a symmetry-breaking phase transition, a finite

ramping rate leads to the generation of topological defects whose density reveals the critical exponents, known as the celebrated Kibble-Zurek mechanism [25–28]. The response of a physical observable to a finite driving rate has also been used to probe intrinsic many-body correlations [29]. Nevertheless, theoretical investigations of the nonadiabatic effect in topological charge pumping are still limited [16,30–32]. Here we would like to understand whether the nonadiabatic effect can characterize the intrinsic properties of this physical system after pumping, such as entanglement generation [33], and whether there exists a reliable way to compute the nonadiabatic effect in an interacting system.

## II. RELATION BETWEEN PURITY AND PUMPING EFFICIENCY

To begin with, let us first discuss an intuition connecting entanglement entropy generated by pumping and the nonadiabatic effect. As shown in Fig. 1, we consider a one-dimensional chain and divide it into left and right halves, whose particle numbers are denoted by  $N_L$  and  $N_R$ , respectively. In the adiabatic limit, a quantized charge is pumped from the left to the right, and the particle numbers become  $N_L - 1$  and  $N_R + 1$ , respectively. However, in the nonadiabatic case, let us denote  $\kappa$  as the pumping efficiency; that is to say, there are certain possibilities, approximated by  $1 - \kappa$ , that the charge is not pumped and the particle numbers remain  $N_L$  and  $N_R$  after a pumping circle, as shown in Fig. 1.

If we take a partial trace over the right system and obtain the reduced density matrix for the left system  $\rho_L$ , we can introduce the second Rényi entropy  $S_2 = -\ln \text{Tr} \rho_L^2$  to describe the entanglement between two sides. Here,  $\text{Tr} \rho_L^2$  is also called the purity, denoted by  $\mathcal{P}$ . For noninteracting-type Gaussian states,

\*huizhai.physics@gmail.com

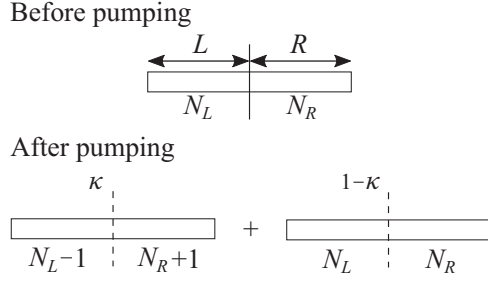


FIG. 1. Schematic of the relation between entanglement or density matrix purity generated by pumping and the pumping efficiency  $\kappa$ .

there exists a formula relating purity with particle numbers. The formula reads [34]

$$\text{Tr} \rho_L^2 = \prod_{p=-1/2}^{1/2} \text{Tr}(\rho_L e^{i\pi p \hat{N}_L}). \quad (1)$$

Using this formula, we obtain

$$\begin{aligned} \mathcal{P} &= \text{Tr} \rho_L^2 \approx \left[ (1 - \kappa) e^{i\frac{\pi}{2} N_L} + \kappa e^{i\frac{\pi}{2} (N_L - 1)} \right] \\ &\quad \times \left[ (1 - \kappa) e^{-i\frac{\pi}{2} N_L} + \kappa e^{-i\frac{\pi}{2} (N_L - 1)} \right] \\ &= (1 - \kappa)^2 + \kappa^2. \end{aligned} \quad (2)$$

This establishes the relation between purity and pumping efficiency. For quantized charge pumping,  $\kappa$  is either unity or zero, leading to  $\mathcal{P} = 1$  and no generation of entanglement entropy. When the nonadiabatic effect occurs,  $\kappa$  can take any value between zero and unity, reducing purity and generating entanglement.

To arrive at this relation, we have assumed that the initial state has fixed particle numbers for both the left and right sides. Strictly speaking, this relation also does not hold when interaction and finite-temperature effects are taken into account. However, we will show that  $\mathcal{P}$  and  $\mathcal{R}$  exhibit the same trend, where  $\mathcal{R}$  denotes  $(1 - \kappa)^2 + \kappa^2$  as the right-hand side of Eq. (2).

Let us denote the probability of transporting  $n$  charges as  $P_n$ . The discussion above only considers  $P_0$  and  $P_1$ . Suppose we would like to consider other possibilities ignored above, and the next order contribution should be two particles being pumped or the backflow of one particle from the right to the left, which are denoted by  $P_2$  and  $P_{-1}$ , respectively. Including all four possibilities and following Eq. (1), we have

$$\mathcal{P} = (P_1 - P_{-1})^2 + (P_0 - P_2)^2. \quad (3)$$

On the other hand, we have the pumping efficiency as

$$\kappa = \sum_n n P_n = 2P_2 + P_1 - P_{-1}, \quad (4)$$

and therefore  $\mathcal{R}$  is given by

$$\mathcal{R} = (2P_2 + P_1 - P_{-1})^2 + (P_0 - P_2 + 2P_{-1})^2. \quad (5)$$

It is easy to verify that

$$\mathcal{R} - \mathcal{P} = 4[P_{-1}P_0 + P_1P_2 + (P_{-1} - P_2)^2] > 0. \quad (6)$$

Hence we further conjecture that  $\mathcal{P} < \mathcal{R}$  as long as the nonadiabatic effect is still perturbative. That is to say, the pumping efficiency provides an upper bound for purity and a lower bound for the entanglement generated during pumping.

### III. RICE-MELE-HUBBARD MODEL AND A SOLVABLE PUMPING CYCLE

The Rice-Mele model is the most widely used model for studying charge pumping [35]. By adding interactions, we consider the Rice-Mele-Hubbard model at half filling [36,37]:

$$\begin{aligned} H &= - \sum_{i,\sigma} (J + (-1)^{i+1} \delta) (c_{i,\sigma}^\dagger c_{i+1,\sigma} + \text{H.c.}) \\ &\quad + \Delta \sum_{i,\sigma} (-1)^{i+1} n_{i\sigma} + U \sum_i n_{i,\uparrow} n_{i,\downarrow}, \end{aligned} \quad (7)$$

where  $n_{i,\sigma} = c_{i,\sigma}^\dagger c_{i,\sigma}$  and  $c_{i,\sigma}$  and  $c_{i,\sigma}^\dagger$  are fermionic annihilation and creation operators.  $J \pm \delta$  is the hopping amplitude between neighboring sites, alternating between two neighboring bonds. The odd and even sites form two sets of sublattices, and  $\Delta$  denotes the energy detuning between them.  $U$  is the on-site interaction strength between different spins. In the pumping process,  $J$ ,  $\delta$ , and  $\Delta$  are functions of time  $t$ . We set  $\hbar = k_B = 1$ , with  $\hbar$  and  $k_B$  being the reduced Planck constant and the Boltzmann constant, respectively.

In the adiabatic limit, for the noninteracting case, a quantized charge pumping can be observed when the trajectory of parameters  $\delta$  and  $\Delta$  encloses the gap-closing point  $\delta = \Delta = 0$  in a pumping circle. This quantized charge pumping is stable in the presence of interaction until the repulsive Hubbard interaction  $U$  exceeds  $2|\Delta_0|$  (see below). Then, the charge pumping breaks down, and the pumped charge is always zero no matter what parameter trajectory is chosen [24,36,37].

Charge pumping with finite driving velocity is a challenging dynamical problem when both interaction and finite-temperature effects need to be considered. To this end, we will introduce a pumping scheme allowing us to compute the dynamics in a numerically exact way. This pumping scheme is illustrated in Fig. 2(a) and contains the following steps:

(1)  $A \rightarrow B$ . We set  $J_0 = J(t=0) = 1$ . All energies are measured in units of  $J_0$ , and the pump velocity  $v$  is measured in units of  $J_0/\hbar$ . We start with  $\delta_0 = \delta(t=0) = 1$ , under which the system forms disconnected double wells. Initially,  $\Delta_0 = \Delta(t=0) < 0$ , and we linearly ramp  $\Delta$  as  $\Delta = \Delta_0(1 - 2vt)$  for a time duration  $t_1 = 1/v$  to  $\Delta = -\Delta_0 > 0$ , with  $J$  and  $\delta$  fixed during the process.

(2)  $B \rightarrow C \rightarrow D$ . We fix  $\Delta = -\Delta_0$  and linearly ramp  $J$  and  $\delta$  to zero as  $J = J_0[1 - v(t - t_1)]$  and  $\delta = \delta_0[1 - v(t - t_1)]$ . In this process we keep the relation  $J = \delta$  such that the system remains as disconnected double wells. When  $t = t_2 = t_1 + 1/v$ , we reach the point  $J = \delta = 0$ , and all sites are disconnected. After that, we ramp up  $J$  as  $J = J_0v(t - t_2)$  and  $\delta$  as  $\delta = -\delta_0v(t - t_2)$  until we reach  $J = J_0$  and  $\delta = -\delta_0$  at  $t_3 = t_2 + 1/v$ . In this process, we always have  $J = -\delta$ , and the system is also disconnected double wells. However, these disconnected double wells are different from those in  $A \rightarrow B \rightarrow C$ . Suppose site  $i$  is connected to site  $(i + 1)$  during  $A \rightarrow B \rightarrow C$ ; then site  $i$  is connected to site  $(i - 1)$  and site  $(i + 1)$  is connected to site  $(i + 2)$  during  $C \rightarrow D$ .

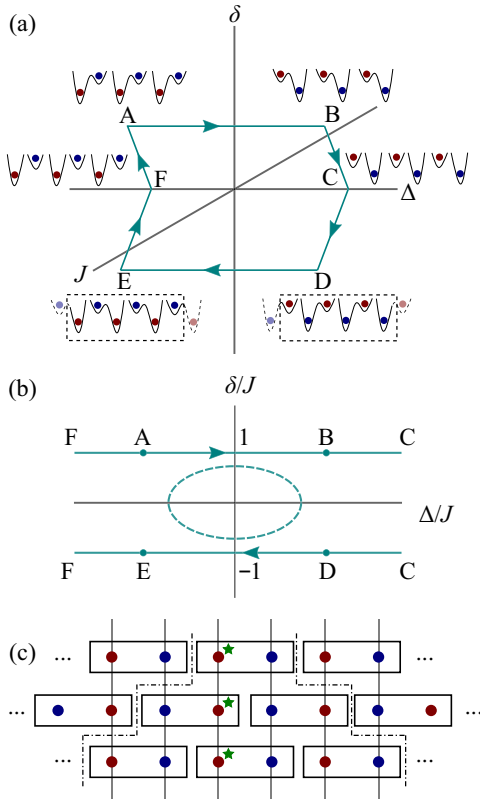


FIG. 2. Illustration of the solvable pumping cycle. (a) The trajectory of the pumping cycle in the  $\delta$ - $\Delta$ - $J$  parameter space. Here,  $B \rightarrow C$  and  $F \rightarrow A$  lines obey  $\delta = J$ , and  $C \rightarrow D$  and  $E \rightarrow F$  lines obey  $\delta = -J$ . The lattice potentials are illustrated at the starting points of each step, where the hopping between two adjacent sites is nonzero (zero) if they are connected (disconnected). (b) The same trajectory as in (a), but shown in the  $(\delta/J)$ - $(\Delta/J)$  parameter space. For comparison, the dashed line shows the conventional topological pumping trajectory, which can be continuously stretched to our trajectory. (c) This pump protocol is represented by a three-layer brick-wall quantum circuit. The first layer represents  $A \rightarrow C$ , the second layer represents  $C \rightarrow F$ , and the third layer represents  $F \rightarrow A$ . The charge transport during one pumping cycle through a given lattice site, say, one marked by a star, can be computed exactly from only six sites within the information light cone denoted by the dash-dotted lines.

(3)  $D \rightarrow E$ . We ramp  $\Delta$  from  $-\Delta_0$  to  $\Delta_0$  with the same velocity  $v$  and by keeping  $J$  and  $\delta$  fixed.

(4)  $E \rightarrow F \rightarrow A$ . This process reverts  $B \rightarrow C \rightarrow D$  with  $\Delta$  fixed. After this step, the parameters return to their initial values, and a pumping cycle is closed.

Intuitively, charge transports from site  $i$  to site  $(i+1)$  from  $A$  to  $B$ . Then, sites  $i$  and  $i+1$  are disconnected, and site  $(i+1)$  is connected to site  $(i+2)$ , which allows subsequently charge transport from site  $(i+1)$  to site  $(i+2)$  during  $D \rightarrow E$ . In such a way, unidirectional charge transport is realized. In this setting, it is straightforward to see that the quantized charge is stable for  $U < 2|\Delta_0|$ .

We remark on the difference between our pumping circle and the conventional ones. Normally, one fixes  $J$  and tunes  $\delta/J$  and  $\Delta/J$  to form a closed loop during a pumping cycle. In the noninteracting case, the pumping is topological or not depending on whether the trajectory loop in the  $(\delta/J)$ - $(\Delta/J)$

diagram encloses zero. As we deform the trajectory, topological pumping remains topological as long as no gap closing occurs in the loop. Here, although we change  $J$  during the pumping, we can still plot the parameter trajectory in the  $(\delta/J)$ - $(\Delta/J)$  diagram, as shown in Fig. 2(b). Especially from  $B$  to  $C$ , it corresponds to fixing  $\delta/J = 1$  and tuning  $\Delta/J$  to positive infinity. Then, from  $C$  to  $D$ ,  $\delta/J$  is fixed to  $-1$ , and  $\Delta/J$  is tuned from infinity to a finite number. In other words, in the  $(\delta/J)$ - $(\Delta/J)$  diagram, we stretch the trajectory loop to  $\Delta/J = \pm\infty$ , and the parameter trajectory becomes two parallel straight lines. However, during this stretching process, no gap closing happens. Hence our pumping cycle is still topologically protected.

A key feature of this designed pumping cycle is that the system is always constituted by disconnected double wells at any given time. Therefore it can be represented by a three-layer brick-wall quantum circuit, as shown in Fig. 2(c). The first layer represents steps  $A$  to  $C$ , the second layer represents steps  $C$  to  $F$ , and the last layer represents steps  $F$  to  $A$ . During one pump cycle, the pumped charge equals the net current passing through any given site. As shown in Fig. 2(c), a given site marked by a star in Fig. 2(c) is only influenced by at most six sites within the light cone, as indicated by the dash-dotted lines in Fig. 2(c). Therefore we only need to compute the six sites by exact diagonalization, and we can obtain an exact result of charge pumping, including interaction, finite driving rate, and finite-temperature effects.

In practice, we compute the current during each step from the change in particle number  $\Delta n$  at a given site  $i$  labeled by a star in Fig. 2(c). Since the system always consists of disconnected double wells, the current and  $\Delta n$  are equal (opposite) when site  $i$  is connected to site  $i-1$  (site  $i+1$ ). When computing the pumped charge, we do not need to assume boundary conditions. As shown in the brick-wall circuit, at any given time the sites outside the light cone denoted by the dash-dotted lines are always disconnected from site  $i$  and do not contribute to  $\Delta n$ . Therefore, diagonalizing the six-site problem is equivalent to solving an infinite chain.

#### IV. RESULTS

With the pumping circle introduced above, typical numerical results on the charge pumping in the Rice-Mele-Hubbard model are shown in Fig. 3. We have fixed  $J_0 = \delta_0 = 1$ ,  $\Delta_0 = -2$ ,  $-7 \leq U \leq 7$ , and  $T = 1$ . We have also varied the temperature range and find that the results are not sensitive to temperature for the parameters we considered.

First, we plot the pump efficiency in Fig. 3(a) for different driving velocities  $v$ . We find two regimes where the pumping efficiency strongly depends on velocity. One regime is  $U < -2|\Delta_0|$ . In this regime, attractive interaction binds two fermions with different spins to form a tightly bound pair, and the hopping of pairs scales as  $\sim 1/|U|$ . Hence, when the interaction is attractive and large, the kinetic energy of fermion pairs becomes small. Therefore a small driving velocity can yield a large deviation. Another regime is  $U \sim 2|\Delta_0|$ . As shown in the inset of Fig. 3(a), when  $U \lesssim 2|\Delta_0|$ , the pumping efficiency  $\kappa$  decreases as  $v$  increases; in contrast, when  $U \gtrsim 2|\Delta_0|$ ,  $\kappa$  increases as  $v$  decreases. Hence, when we plot  $\kappa$  as a function of  $U$  for different  $v$ , these curves cross nearly at the

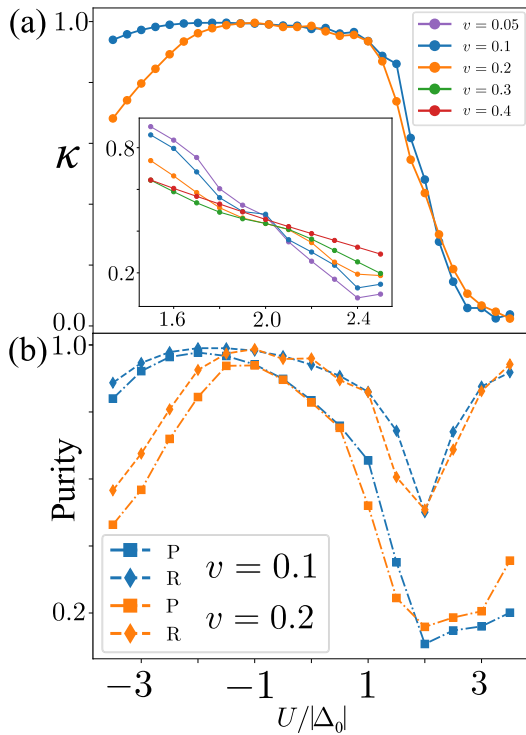


FIG. 3. Numerical results of charge pumping for the Rice-Mele-Hubbard model using the solvable pumping circle shown in Fig. 2. Here we fix  $J_0 = \delta_0 = 1$ ,  $\Delta_0 = -2$ , and temperature  $T = 1$ . (a) The pump efficiency  $\kappa$  as a function of  $U/|\Delta_0|$  for various driving speeds  $v$ . The inset shows a zoomed-in plot around  $U = 2|\Delta_0|$  where the pumping efficiencies with different driving velocities nearly cross at a single point. (b) Comparison between purity  $\mathcal{P}$  and  $\mathcal{R} = (1 - \kappa)^2 + \kappa^2$  for two different driving velocities.

same point  $U = 2|\Delta_0|$ . This point marks the transition from topological to nontopological charge pumping in the adiabatic limit, which is rooted in the ground state phase transition from a band insulator to a Mott insulator at  $U = 2|\Delta_0|$ . In other words, we show that even with the experimental data measured at finite velocity, one is able to accurately locate the transition point of quantized charge pumping in the adiabatic limit.

Here we should also note the difference between pumping efficiency and the deviation from quantization. When  $U \lesssim 2|\Delta_0|$ , topological pumping is quantized to unity, and  $\kappa$  is always greater than 0.5. The deviation is  $1 - \kappa$ . When

$U \gtrsim 2|\Delta_0|$ , pumping is quantized to zero in the adiabatic limit, and the deviation is  $\kappa$ , which is always smaller than 0.5. The largest deviation from quantization is 0.5 occurring at  $U = 2|\Delta_0|$ , where  $\mathcal{R}$  reaches its minimum at 0.5.

Finally, in Fig. 3(b), we support our conjecture that  $\mathcal{P} < \mathcal{R}$ . When computing the purity, we assume the open boundary condition. We compare  $\mathcal{P}$  and  $\mathcal{R}$  for two different driving velocities,  $v = 0.1$  and  $v = 0.2$ . We have calculated the results for a number of different temperatures and velocities. All results are similar and so are not repeatedly shown here. We can see that  $\mathcal{R}$  also decreases significantly as  $v$  increases in the regime  $U < -2|\Delta_0|$ . Meanwhile,  $\mathcal{R}$  exhibits a minimum around  $U \approx 2|\Delta_0|$  where the deviation from quantization is the largest. This shows that  $\mathcal{P}$  and  $\mathcal{R}$  exhibit the same trend. Meanwhile, we also see that  $\mathcal{P}$  is always smaller than  $\mathcal{R}$ .

## V. CONCLUSION

In summary, we propose a pumping scheme that allows us to compute charge pumping for interacting cases in a numerically exact way. This scheme is also equivalent to a quantum circuit model, potentially bringing out the connection between charge pumping and digital quantum computing. We discuss the connection between deviation from quantization and generation of entanglement, both rooted in nonadiabatic dynamics. We also note that the relation between charge transport and entanglement has also been noticed in quantum point contact [38] and recently in quantized nonlinear conductance [2,34,39,40]. All these phenomena might point to a unified picture behind them.

The open-source code is available [41].

## ACKNOWLEDGMENTS

We thank Pengfei Zhang, Haifeng Tang, Chengshu Li, Minggen He, Wei Zheng, Chang Liu, and Tianshu Deng for helpful discussions. The project is supported by Beijing Outstanding Young Scholar Program, Innovation Program for Quantum Science and Technology Grant No. 2021ZD0302005, NSFC Grant No. 11734010, and the XPLORER Prize. F.Y. is also supported by Chinese International Postdoctoral Exchange Fellowship Program (Talent-Introduction Program) and Shuimu Tsinghua Scholar Program at Tsinghua University.

[1] R. Landauer, Spatial variation of currents and fields due to localized scatterers in metallic conduction, *IBM J. Res. Dev.* **1**, 223 (1957).  
 [2] C. L. Kane, Quantized nonlinear conductance in ballistic metals, *Phys. Rev. Lett.* **128**, 076801 (2022).  
 [3] K. V. Klitzing, G. Dorda, and M. Pepper, New method for high-accuracy determination of the fine-structure constant based on quantized Hall resistance, *Phys. Rev. Lett.* **45**, 494 (1980).  
 [4] D. C. Tsui, H. L. Stormer, and A. C. Gossard, Two-dimensional magnetotransport in the extreme quantum limit, *Phys. Rev. Lett.* **48**, 1559 (1982).

[5] F. D. M. Haldane, Model for a quantum Hall effect without Landau levels: Condensed-matter realization of the ‘‘parity anomaly’’, *Phys. Rev. Lett.* **61**, 2015 (1988).  
 [6] C.-Z. Chang, J. Zhang, X. Feng, J. Shen, Z. Zhang, M. Guo, K. Li, Y. Ou, P. Wei, L.-L. Wang, Z.-Q. Ji, Y. Feng, S. Ji, X. Chen, J. Jia, X. Dai, Z. Fang, S.-C. Zhang, K. He, Y. Wang *et al.*, Experimental observation of the quantum anomalous Hall effect in a magnetic topological insulator, *Science* **340**, 167 (2013).  
 [7] C.-X. Liu, S.-C. Zhang, and X.-L. Qi, The quantum anomalous Hall effect: Theory and experiment, *Annu. Rev. Condens. Matter Phys.* **7**, 301 (2016).

- [8] C.-Z. Chang, C.-X. Liu, and A. H. MacDonald, Colloquium: Quantum anomalous Hall effect, *Rev. Mod. Phys.* **95**, 011002 (2023).
- [9] C. L. Kane and E. J. Mele, Quantum spin Hall effect in graphene, *Phys. Rev. Lett.* **95**, 226801 (2005).
- [10] B. A. Bernevig, T. L. Hughes, and S.-C. Zhang, Quantum spin Hall effect and topological phase transition in HgTe quantum wells, *Science* **314**, 1757 (2006).
- [11] M. König, S. Wiedmann, C. Brune, A. Roth, H. Buhmann, L. W. Molenkamp, X.-L. Qi, and S.-C. Zhang, Quantum spin Hall insulator state in HgTe quantum wells, *Science* **318**, 766 (2007).
- [12] J. Maciejko, T. L. Hughes, and S.-C. Zhang, The quantum spin Hall effect, *Annu. Rev. Condens. Matter Phys.* **2**, 31 (2011).
- [13] R. B. Laughlin, Quantized Hall conductivity in two dimensions, *Phys. Rev. B* **23**, 5632 (1981).
- [14] D. J. Thouless, Quantization of particle transport, *Phys. Rev. B* **27**, 6083 (1983).
- [15] Q. Niu and D. J. Thouless, Quantised adiabatic charge transport in the presence of substrate disorder and many-body interaction, *J. Phys. A: Math. Gen.* **17**, 2453 (1984).
- [16] Q. Niu, Towards a quantum pump of electric charges, *Phys. Rev. Lett.* **64**, 1812 (1990).
- [17] D. Xiao, M.-C. Chang, and Q. Niu, Berry phase effects on electronic properties, *Rev. Mod. Phys.* **82**, 1959 (2010).
- [18] R. Citro and M. Aidelsburger, Thouless pumping and topology, *Nat. Rev. Phys.* **5**, 87 (2023).
- [19] M. Lohse, C. Schweizer, O. Zilberberg, M. Aidelsburger, and I. Bloch, A Thouless quantum pump with ultracold bosonic atoms in an optical superlattice, *Nat. Phys.* **12**, 350 (2016).
- [20] S. Nakajima, T. Tomita, S. Taie, T. Ichinose, H. Ozawa, L. Wang, M. Troyer, and Y. Takahashi, Topological Thouless pumping of ultracold fermions, *Nat. Phys.* **12**, 296 (2016).
- [21] H. I. Lu, M. Schemmer, L. M. Ayccock, D. Genkina, S. Sugawa, and I. B. Spielman, Geometrical pumping with a Bose-Einstein condensate, *Phys. Rev. Lett.* **116**, 200402 (2016).
- [22] J. Tangpanitanon, V. M. Bastidas, S. Al-Assam, P. Roushan, D. Jaksch, and D. G. Angelakis, Topological pumping of photons in nonlinear resonator arrays, *Phys. Rev. Lett.* **117**, 213603 (2016).
- [23] D. Dreon, A. Baumgärtner, X. Li, S. Hertlein, T. Esslinger, and T. Donner, Self-oscillating pump in a topological dissipative atom-cavity system, *Nature (London)* **608**, 494 (2022).
- [24] A.-S. Walter, Z. Zhu, M. Gächter, J. Minguzzi, S. Roschinski, K. Sandholzer, K. Viebahn, and T. Esslinger, Quantisation and its breakdown in a Hubbard-Thouless pump, *Nat. Phys.* **19**, 1471 (2023).
- [25] T. W. B. Kibble, Topology of cosmic domains and strings, *J. Phys. A: Math. Gen.* **9**, 1387 (1976).
- [26] T. W. B. Kibble, Some implications of a cosmological phase transition, *Phys. Rep.* **67**, 183 (1980).
- [27] W. Zurek, Cosmological experiments in superfluid helium, *Nature (London)* **317**, 505 (1985).
- [28] A. del Campo and W. H. Zurek, Universality of phase transition dynamics: Topological defects from symmetry breaking, *Int. J. Mod. Phys. A* **29**, 1430018 (2014).
- [29] L. Liang, W. Zheng, R. Yao, Q. Zheng, Z. Yao, T.-G. Zhou, Q. Huang, Z. Zhang, J. Ye, X. Zhou, X. Chen, W. Chen, H. Zhai, and J. Hu, Probing quantum many-body correlations by universal ramping dynamics, *Sci. Bull.* **67**, 2550 (2022).
- [30] W.-K. Shih and Q. Niu, Nonadiabatic particle transport in a one-dimensional electron system, *Phys. Rev. B* **50**, 11902 (1994).
- [31] L. Privitera, A. Russomanno, R. Citro, and G. E. Santoro, Nonadiabatic breaking of topological pumping, *Phys. Rev. Lett.* **120**, 106601 (2018).
- [32] A. Grabarits, A. Takács, I. C. Fulga, and J. K. Asbóth, Floquet-Anderson localization in the Thouless pump and how to avoid it, [arXiv:2309.12882](https://arxiv.org/abs/2309.12882).
- [33] R. Gawatz, A. C. Balram, E. Berg, N. H. Lindner, and M. S. Rudner, Prethermalization and entanglement dynamics in interacting topological pumps, *Phys. Rev. B* **105**, 195118 (2022).
- [34] P. M. Tam, M. Claassen, and C. L. Kane, Topological multipartite entanglement in a Fermi liquid, *Phys. Rev. X* **12**, 031022 (2022).
- [35] M. J. Rice and E. J. Mele, Elementary excitations of a linearly conjugated diatomic polymer, *Phys. Rev. Lett.* **49**, 1455 (1982).
- [36] M. Nakagawa, T. Yoshida, R. Peters, and N. Kawakami, Breakdown of topological Thouless pumping in the strongly interacting regime, *Phys. Rev. B* **98**, 115147 (2018).
- [37] E. Bertok, F. Heidrich-Meisner, and A. A. Aligia, Splitting of topological charge pumping in an interacting two-component fermionic Rice-Mele Hubbard model, *Phys. Rev. B* **106**, 045141 (2022).
- [38] I. Klich and L. Levitov, Quantum noise as an entanglement meter, *Phys. Rev. Lett.* **102**, 100502 (2009).
- [39] F. Yang and H. Zhai, Quantized nonlinear transport with ultracold atoms, *Quantum* **6**, 857 (2022).
- [40] P. Zhang, Quantized topological response in trapped quantum gases, *Phys. Rev. A* **107**, L031305 (2023).
- [41] <https://github.com/YangFan403/ChargePump>.